SAFIR: A Thermal/Structural Program for Modeling Structures Under Fire

JEAN-MARC FRANSSEN

This paper was presented at the 2003 North American Steel Construction Conference.

When it comes to evaluating the behavior of building structures subjected to fire, numerical modeling using computers is known to present several advantages compared to experimental testing. The high cost and the amount of time required to prepare and to perform a test were among the main problems on the table when the first tools for modeling structures in fire were developed. The primary objective at that time was to perform numerically the tests that were previously possible only in the laboratories. It quickly became obvious that these numerical tools offer other benefits. One is the ability to analyze the behavior of complete structures—as opposed to simple elements—with huge sizes that cannot fit in a full-scale furnace and with very complex load redistribution phenomena that are completely ignored when testing single elements. Another benefit is the ability to perform parametric analyses, because the variability associated with experimental testing is not present in numerical modeling; it is therefore much easier to highlight the influence of any chosen parameter on the final result. Nowadays, these tools are mainly used either for the design of complex structures in real projects or for the development and verification of more simple design methods to be used in everyday practice for more simple elements.

The discipline of *Structures-in-Fire Modeling,* or *SiF Modeling*, has developed quite significantly during the last decades and is still currently the subject of important research efforts around the world. It is nowadays an essential part of the science of fire safety engineering. It has yet to be realized that, as for any other discipline, it has its own limits that the user has to know and respect when analyzing a structure. Also, when developing new materials or new construction systems for example, experimental testing will probably remain forever an essential part of the process.

Jean-Marc Franssen is associate professor, University of Liege, Liege, Belgium.

HISTORY

Three families of computer software used in SiF modeling can be distinguished.

- One comprises all the software that were specifically written in order to model one very specific and particular type of element subjected to fire such as steel beams, concrete walls, or concrete columns. All of these are proprietary programs, usually established by individual researchers, typically for the purpose of their Ph.D. All have their own merits, but they will never be able to allow the analysis of any other element than the one for which they have been made, and most of them have seen their development stopped after a while.

- On the other side is commercial software. They have not been developed with the objective of modeling structures in fire, but they offer numerous possibilities, have great pre- and post-processing capabilities and have normally received extensive attention for their validation. The price may yet be a problem, although some education licenses are usually offered for research purposes, and it is not so straightforward to become familiar with all the possibilities that have to be utilized in order to perform a SiF modeling analysis. On the condition that the user is familiar with a particular software, it is possible to constrain or squeeze such software in such a way that it performs a perfectly sound analysis of a structure in a fire. One of the problems is that any user who is familiar with the code will end up with some results and with nice drawings, but a solid education and a high level of experience in structural mechanics, in thermal problems, in nonlinear modeling and finally in the behavior of structures in fire are also required before any confidence can be put in these results. This is also the case for the two other families of software but, for these other two, it comes as evidence because these tools are specifically designed for the SiF situation and, as a consequence, they are normally used only by SiF experts.

- An intermediate situation between commercial codes and very specific software is that of the software that have been developed specifically with the objective of model-

ing structures in fire, but where efforts have been made to have a wider and more general field of application. They normally offer a library of different material models and of different finite elements that can be combined to adapt to different situations and structures. They typically result from a succession of numerous different Ph.D. theses and research projects performed in a university department that has SiF as its main research activity. Most of them are still confined to the research center where they are developed, although there is a recent tendency for these tools to be used also by other research centers or by design offices that specialize in fire safety engineering.

The objective of this paper is the presentation of the numerical software SAFIR that has been developed over the last 20 years at the University of Liege in Belgium. It belongs to the intermediate family because it has been specifically written in order to allow modeling of the behavior of structures subjected to fire, but care has been taken to have a field of application that would be as wide as possible.

Among the first attempts to model numerically the behavior of structures subjected to fire are the works done in the United States (U.S.) at Berkeley where the team of Bresler developed the software FIRES-T (Becker, Bizri, and Bresler, 1974a) and FIRES-RC (Becker, Bizri, and Bresler, 1974b) for the analysis of reinforced concrete elements. These programs have later received a wider field of application owing to developments introduced mainly by Iding; names of the second versions are FIRES-T3 (Iding, Bresler, and Nizamuddin, 1977a) and FIRES-RCII (Iding, Bresler, and Nizamuddin, 1977b). Iding later wrote software for the analysis of steel floor systems (Iding and Bresler, 1980). For reasons unknown to the author of this paper, it seems as if the interest for SiF modeling decreased progressively in the U.S. and most of the activity in the field since the 1980s has occurred in Europe.

At the University of Liege, the subject of SiF modeling was first investigated by Dotreppe who, after a period spent at the University of Illinois, first presented in Liege a Ph.D. thesis on the finite element analysis of reinforced concrete slabs until failure at ambient temperature (Dotreppe, 1972). The possibility to take the fire action into account was later introduced in his post-doctoral research (Dotreppe, 1980). The software written at that time allowed determination of the 2D transient thermal field in a rectangular reinforced concrete section. A rectangular mesh was used for the finite difference scheme utilized, widely based on a previous program published in France (Coin, 1976). Although the mechanical analysis was limited to simply supported rectangular reinforced concrete beams and did not take the effects of large displacements into account, the principle of the division of the section into fibers with a different temperature in each fiber—the fiber model—was already present. This principle is still used in the most recent version of the beam finite element model of SAFIR.

In the beginning of the 1980s, the steel producer, ARBED, now part of the ARCELOR group, thought that one possible solution to steel fire resistance could lay in the composite steel-concrete assemblies. Numerical modeling was quickly recognized as the only option for determining the temperature distribution as well as the mechanical behavior of such elements and, with financial support of the ECSC, ARBED commissioned the University of Liege for the development, by the author of this paper working under supervision of Dotreppe, of software that received the name of CEFICOSS. The first presentation (Schleich, Dotreppe, and Franssen, 1986) was made at the first International Association for Fire Safety (IAFSS) conference held at the National Institute of Standards and Technology (NIST) in the U.S. and more detailed information is given in the Ph.D. thesis of the author (Franssen, 1987). The mechanical model was based on a 2D Bernoulli beam finite element taking large displacements into account and with a discretisation of the section utilizing the fiber model. Because either steel or concrete material can be present in each mesh of the section, this software allows the analysis of pure steel, reinforced concrete, or composite steel-concrete 2D framed structures. The determination of the temperatures in the section is still based on a finite difference scheme and a rectangular meshing. This software CEFICOSS has been used in numerous European funded theoretical research projects, for the preliminary design of experimental tests to be performed as well as for the design of hundreds of real buildings. It was still in use recently and is considered as a valid and very useful tool for problems that are in its field of application. This software has never been distributed outside the research center of ARBED.

When it became clear that ARBED had more interest in utilizing the existing CEFICOSS software than in further developments, the author of this paper decided, in the frame of his scientific career within the National Fund for Scientific Research, to start the development of a totally new SiF software that would include, from the beginning, some possibilities that are missing and that would be impossible to implement in CEFICOSS. This new software, SAFIR, would serve as a general platform allowing further developments, either be it in the library of finite elements or in the constitutive models. It was also decided that this software should run on a personal computer in a Windows environment, because of the facility for doing developments in graphics output and because of the portability offered by a widely utilized operating system.

OVERVIEW

The main objective of a SiF analysis is to determine the mechanical behavior of a structure during a fire until failure; this determination will be called here the mechanical analysis.

Table 1. Link Between the Thermal and the Mechanical Analysis	
Thermal analysis	Mechanical analysis
2D analysis on the section	2D or 3D beam finite element
1D analysis on the thickness	3D shell finite element
3D user defined temperature field	
Uniform temperature by a simple model	2D or 3D truss finite element
3D analysis	Simple model

It is generally accepted that, as opposed to determining the ultimate load bearing capacity of the structure after a certain duration of fire, it is preferable to track the behavior of the structure minute-by-minute during the whole development of the fire.

It is therefore necessary to have the knowledge of the temperature distribution in the structure during the whole course of the fire. One possibility is to rely on separate software for the determination of this temperature distribution, called here the thermal analysis. This method can lead to interface problems when the results of one program, in other words, the temperatures, have to be passed to the other program. In SAFIR, the same software is used for both the thermal and the mechanical analysis and great care has been taken in order to have an automatic transmission of information from one analysis to the other.

The thermal analysis and the mechanical analysis are nevertheless performed separately and subsequently, which means that the temperature distribution will obviously deeply influence the mechanical response, but the opposite is not true; there is, for example, no influence of the cracking of concrete determined in the mechanical analysis on the thermal conductivity that is used in the thermal analysis.

The determination of the temperatures in the fire compartment is not considered as part of the SiF analysis. This determination must have been done previously and the information, either in terms of gas temperature or in terms of heat flux, is used as input data in the thermal part of the SiF analysis.

The interconnection between the thermal analysis and the mechanical analysis is therefore a key factor in the user friendliness of this software. The type of thermal analysis that is performed depends of course directly on the type of mechanical analysis that will be performed subsequently. Table 1 shows the links that exist between the thermal and the mechanical analyses.

- If a beam finite element is used in the mechanical analysis, be it either a 2D or a 3D beam element, a 2D thermal analysis is performed in order to determine the temperature distribution on the cross section of the beam. This means that no heat flux is considered along the longitudinal axis of the beam finite element.

- If a shell finite element is used in the mechanical analysis, the standard procedure is to assume that the temperature varies only on the thickness of the slab as is the case, for example, in a reinforced concrete slab. This temperature distribution across the thickness could theoretically be determined by using uniaxial elements in the thermal analysis. In fact, because no such elements are programmed in the software, 2D rectangular elements are used to analyze a width of, say, 1 cm and only the necessary amount of information is stored, in other words, only the temperature in one out of every two nodes used in the discretization.

- Another possibility has been introduced more recently for the user to introduce a temperature distribution in the shell elements that varies not only across the thickness but also in the plane of the elements. This is done by a *Dynamic Link Library* procedure that the user has to write and compile separately.

- If a truss finite element is used in the mechanical analysis, this is mainly to represent slender steel elements in tension such as, for example, external tendons in prestressed structures or suspension rods. It is then assumed that the temperature is uniform on the section of the element and this temperature can be determined by simple calculation models based on the hypothesis of uniform temperature and on the massivity factor.

- The software also allows 3D thermal analysis but, in this case, there is no possibility to pursue directly with a mechanical analysis based on 3D solid, or brick, finite elements. The information obtained on the temperature distribution can be used in the estimation of the load bearing capacity made in a simple design method such as, for example, the hand calculations based on the strut-and-tie model for reinforced concrete structures.

When a 3D beam finite element is used, the torsional stiffness of the section is required in order to build the stiffness matrix. Except for some typical sections made of one material only, the user does not know this property. SAFIR can determine the torsional stiffness of a section with any shape and comprising several different materials, see the section entitled "The Torsion Analysis". The elastic stiffness at 20 °C is computed and the user can decide to consider only a part of this value during the mechanical analysis because of the reduction that can take place due to, for example, cracking in concrete or to temperature increase.

THE THERMAL ANALYSIS

Basic Equations

Heat transfer by conduction in solid materials is described by the Fourier equation that is solved in SAFIR according to the standard finite element procedure (see Appendix). The main hypotheses are:

- the materials are isotropic, not submitted to movements, not compressible and have no mechanical dissipation,
- no contact thermal resistance exist at the interface between adjacent materials.

Linear isoparametric finite elements are used in order to represent the geometry, based on the coordinates of the nodes, and the temperature distribution, based on the temperature at the nodes. In a 2D analysis with SAFIR, triangles and quadrangles can be used whereas 6-noded and 8-noded elements can be used in a 3D analysis (see Figure 1).

Heat exchanges in internal cavities can also be taken into account according to the same principles as those described by Wickström (1979). The main hypotheses are:

a. Heat transfer in the cavity by conduction in the gas is negligible.

b. Specific heat of the gas in the cavity is negligible.

c. The gas in the cavity is transparent. It does not absorb radiation energy.

d. The boundaries of the cavity are gray surfaces.

Because of hypotheses a, b, and c, and if convection transfer is assumed to be linearly temperature dependent, the temperature of the gas in the cavity is unique and is at any time equal to the average of the temperatures on the border of the cavity, in other words, equal to the weighted average of the temperature of the nodes around the cavity. The temperature of the gas is used to calculate heat exchanges by convection. This mode of heat transfer is usually much less significant than the radiation between the internal surfaces of the cavity.

The radiation heat transfer in a nonparticipating media is based on the concept of radiosity and irradiation as explained, for example, by Tien, Lee, and Stretton (1995). The border of the cavity is divided into a finite number of gray diffuse surfaces, each being one side of a finite element.

The irradiation, G_i, is the radiative flux reaching a surface I, as given by Equation 1.

$$G_i = F_{ij} J_j \tag{1}$$

where

F_{ij} = view factor from surface i to surface j

The surface radiosity, J_i, is the total radiative flux, including emission and reflection, leaving the surface j. Taking into account Kirchoff's law on a gray surface, it is given by Equation 2.

$$J_i = \sigma \varepsilon^*_{(i)} T_i^4 + \left(1 - \varepsilon^*_{(i)}\right) G_i \tag{2}$$

where

σ = Stefan-Boltzman coefficient, 5.67×10^{-8} W/m^{2}K^4

$\varepsilon^*_{(i)}$ = relative emissivity of the material. The parentheses around i mean that i is not an indices of summation in this case, as it was in Equation 1.

The net flux, q_i, leaving the surface i is given by Equation 3.

$$q_i = \sigma \varepsilon^*_{(i)} T_i^4 - \varepsilon^*_{(i)} G \tag{3}$$

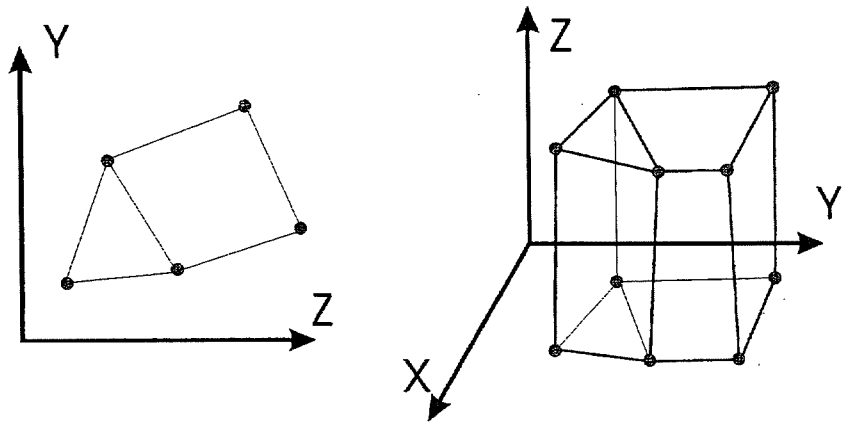

Fig. 1. Finite elements for the thermal analyses.

Introducing Equations 1 and 2 into Equation 3 yields Equation 4.

$$\left\{\frac{F_{ij}\left(1-\varepsilon_{(j)}\right)}{\varepsilon_{(j)}}-\frac{\delta_{ij}}{\varepsilon_{(j)}}\right\}q_j = F_{ij}\,\sigma T_j^4 - \sigma T_i^4 \qquad (4)$$

This equation, when the flux are transformed into energy and when the matrix in the left hand term is inverted, yields a relation that allows calculating the energy leaving every surface as a function of the fourth power of the temperatures at the nodes of the border of the cavity.

The view factors are calculated once at the beginning of the calculation by SAFIR according to the rule of Hottel (1954). The energy derived from Equation 4 is taken into account in the evaluation of the residue, Equation 11 in the Appendix, but is not taken into account in the iteration matrix, Equation 14 in the Appendix, because the third power terms would make a totally non-symmetric matrix and also because this would link some nodes that are geometrically distant from each other and would destroy the sparse, or band, character of the matrix. The fact that the iteration matrix does not include the effects of the radiation may slightly increase the number of iterations required for convergence, but the convergence is still toward the true solution because the effect of radiation is duly taken into account in the residue.

Capabilities and Limitations of the Software

Different material properties can be used in the same structure, but there is only one material in each finite element. The temperature dependent thermal properties of different materials have been programmed in the code: Eurocode 2 (concrete) (Eurocode, 1995b), Eurocode 3 (steel) (Eurocode, 1995c), Eurocode 9 (aluminum) (Eurocode, 1998), and gypsum. One material with constant thermal properties and five materials with linear temperature dependent thermal conductivity, specific heat, and specific mass defined by the user can also be used.

It is possible to take into account the energy dissipated by the evaporation of free water, in concrete for example. The user simply gives the amount of free water in kg/m³. This energy is released at a constant rate from 100 °C to 115 °C, and then the energy release rate is linearly decreasing from 115 °C to 200 °C. Another option is to introduce this energy, or any other energy release due to, for example, possible chemical reactions, into the curve giving the evolution of the specific heat. The algorithm is in fact based on the computation of the enthalpy instead of the specific heat because this makes the software much more stable in cases where the specific heat curve shows sudden and severe variations as is the case, for example, in gypsum.

Different boundary conditions can be introduced, as follows:

- The user can prescribe the evolution of the temperature as a function of time at different nodes. This can be used mainly for validation purposes by comparison with academic examples (Pintea and Franssen, 1997) or if the temperature evolution has been recorded in a laboratory test at particular locations in the section, say, on the rebar, and the user wants this temperature evolution to be respected in the numerical result.

- The heat flux at the boundary can be directly imposed as a function of time by the user. At the moment, this possibility has only been programmed for 2D analyses.

- An adiabatic boundary condition is imposed *de facto* if no boundary condition is given at a border. This is used to model an axis of symmetry. In the solution, the isotherms will be perpendicular to this boundary.

- The heat flux exchanged between a boundary and the hot gas in a fire compartment can be modeled according to the recommendation of Eurocode 1 (Eurocode, 1995a), with a linear convective term and a radiation term, see Equation 5.

$$q_n = h\left(T_g - T_S\right) + \sigma\varepsilon^*\left(T_g^4 - T_S^4\right) \qquad (5)$$

where

h = coefficient of convection, W/m²-K
T_g = temperature of the gas, given in the data as a function of time, K
T_S = temperature on the boundary of the structure, K

Complex algorithms have been introduced that allow consideration of radiation in 2D cavities even if the shape of the cavity is very complex, with some surfaces bonding the cavity not seeing each other, or seeing each other only partially because the cavity is concave. An object can be included in the cavity while not touching the border of the cavity, as would be the case, for example, for a steel rolled column encased in a circular stainless steel tube used for decorative purposes. The cavity can even separate two objects that do not touch each other as, for example, a false ceiling under a concrete or composite concrete slab. More details on this are given by Franssen (2003).

The time step has to be chosen by the user, based on his experience. Values typically used at the beginning of the test are, for example, 1 second if gypsum material is present, and 10 seconds otherwise, although surprisingly good results have been found in concrete assemblies with time steps as long as 1800 seconds.

Apart from operational limitations, such as the fact that radiations in cavities and imposed heat flux boundary

conditions have only been programmed in 2D sections, the main limitations of the program are linked to the main hypotheses.

- Contact is assumed to be perfect between two adjacent materials; there is no resistance to heat transfer by conduction at the interface between two adjacent elements with different materials.

- The geometry is fixed during the duration of the simulation. For example, the effects of spalling or the detachment of gypsum boards from the studs of compartment walls cannot be modeled easily. It is indeed possible for the user to adapt the geometry at a given time, reducing for example the thickness of an insulation layer or suppressing the concrete cover on the reinforcing bars, and to restart the analysis with the new geometry. The temperatures obtained in the initial geometry at that time are taken as new initial conditions for the subsequent analysis. At what time this modification of the geometry has to be done and the amount of material that has to be suppressed is nevertheless not given by the analysis, the user has to exercise engineering judgment and make a decision.

- Moisture movements are not taken into account.

- There is no influence of the stress distribution on the thermal analysis; cracking in concrete, for example, will not create anisotropy in the thermal properties.

- The knowledge of thermal properties of insulating materials is very often limited, especially in the high temperatures range.

- It remains a challenge to make a good interface between the environment in the fire compartment and the structure when the fire is localized and a single temperature in the compartment can thus not represent the situation. If, for example, the situation in the compartment has been analyzed by a computational fluid dynamic numerical program, the result will be made of gas temperatures and heat fluxes in various directions in the thousands of cells used to represent the compartment. The transfer of all this information to the finite element code is far more complex than simply using Equation 5 with a single gas temperature.

Examples

Figure 2 shows the discretization of a prefabricated system made of hot-rolled steel sections; one can be seen in the center of the picture. Prefabricated short terracotta elements are placed on the lower flange of adjacent steel sections and a concrete layer is added on top. Finally, a layer of gypsum is applied underneath the system. The temperatures determined in this section could be used, for example, in a mechanical analysis using 2D beam finite elements.

Figure 3 shows the temperature distribution after 90 minutes of an ISO fire (1999) in one half of the web of a reinforced concrete beam with circular openings. This temperature field has been used in the evaluation of the shear capacity using a simple strut-and-tie model.

THE MECHANICAL ANALYSIS

Basic Equations

The basis of the mechanical analysis of structures undergoing large displacements is the incremental form of the prin-

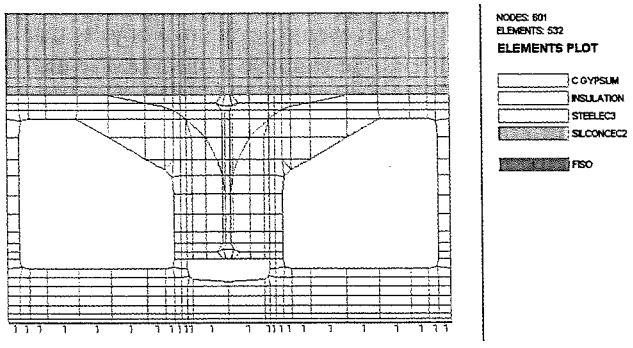

Fig. 2. Part of an old prefabricated flooring system.

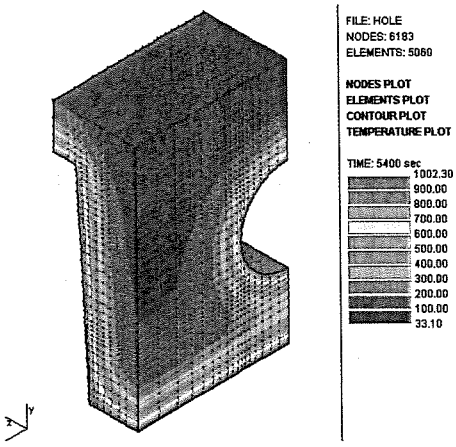

Fig. 3. Concrete beam with circular openings.

cipal of virtual work. If a total co-rotational configuration is used, it is given by Equation 6 in which the forces applied on the surface of the structure have not been considered.

$$\int_V \left(\bar{D}_{ijkl}\, d\bar{E}_{kl}\, \delta\bar{E}_{ij} + S_{ij}\, \delta d\bar{E}_{ij} \right) dV = \int_V \left(d\bar{f}_i\, \delta\bar{u}_i + \bar{f}_i\, \delta d\bar{u}_i \right) dV \qquad (6)$$

Any variable in Equation 6 that appears with a bar, such as $\bar{D}_{ijkl}$, is evaluated not from the initial position of the element but from a position obtained by a rigid body movement that translates the undeformed element as close as possible to the deformed position:

where

$V = \bar{V}$ = the undeformed volume of the element

S_{ij} = tensor of the second Piola-Kirchoff stress

$\bar{D}_{ijkl} = D_{ijkl}$ = tensor defining the incremental constitutive law of the material, see Equation 7

$\delta\bar{E}_{ij}$ = tensor of the Green virtual field of displacement, see Equation 8

$\bar{f}_i$ = volume forces

$\delta\bar{u}_i$ = virtual field of displacements from the deformed position of the element

In a material where the temperatures change during the simulation, the constitutive law is given by Equation 7.

$$dS_{ij} = D_{ijkl} \left(dE_{kl} - dE_{kl}^{th} \right) = D_{ijkl}\, dE_{kl}^{m} \qquad (7)$$

where

dE_{kl}^{th} = tensor of incremental thermal strain

dE_{kl}^{m} = tensor of mechanical, or stress-related, strains

Equation 8 gives the tensor of Green of the virtual field of displacement.

$$\delta\bar{E}_{ij} = \frac{1}{2} \left(\delta\bar{u}_{i,j} + \delta\bar{u}_{j,i} + \bar{u}_{k,i}\, \delta\bar{u}_{k,j} + \delta\bar{u}_{k,i}\, \bar{u}_{k,j} \right) \qquad (8)$$

In order to solve Equation 6 in a displacement based finite element formulation, the field of displacements is represented in an approximate manner by the discretized field **u** that depends on the displacements of the nodes **p** via appropriately chosen shape functions **N**, see Equation 9 written in a matrix form.

$$\mathbf{u} = \mathbf{N}\mathbf{p} \qquad (9)$$

This allows the incremental tensor of strains to be derived also as a function of the nodal displacements, see Equation 10 in which the matrix **B** contains not only spatial derivatives of the shape functions as in a small deformations formulation, but also the nodal displacements that are not identically equal to 0 in the co-rotated configuration.

$$d\mathbf{e} = \mathbf{B}\, d\mathbf{p} \qquad (10)$$

The matrix equation that governs the iteration from one position to the next position of equilibrium is Equation 11.

$$\int_v \mathbf{B}^T\, \mathbf{D}\mathbf{B}\, dV\, d\mathbf{p} + \int_v \mathbf{S}^T\, \delta d\mathbf{e}\, dV\, d\mathbf{p} = \left(\mathbf{K}_u + \mathbf{K}_s \right) d\mathbf{p} = \mathbf{f}^{ext} - \mathbf{f}^{int} \qquad (11)$$

where

$\mathbf{K}_u$ comprises the linear elastic and the geometric stiffness matrices

$\mathbf{K}_s$ is the stress generated stiffness matrix

The nodal forces energetically equivalent to the applied forces, $\mathbf{f}^{ext}$, and the nodal forces obtained from integration of the internal stresses, $\mathbf{f}^{int}$, are also obtained from the principle of virtual work via similar considerations that are not given here for reasons of space. See Franssen (1997).

The Truss Finite Element

The element has a constant section of area A along the longitudinal axis that is a straight line extending between the two end nodes. The axial displacement along the element is thus linear and the strain is constant, given by Equation 12:

$$E_{xx} = \frac{L^2 - L_0^2}{L_0^2} \qquad (12)$$

where

L = length of the deformed element

L_0 = initial length of the element

The internal nodal force f_x produced by the axial stress S_{xx} is given by Equation 13.

$$f_x^{int} = -A\, S_{xx}\, \frac{L}{L_0} \qquad (13)$$

Finally, the two stiffness matrices are given by Equations 14 and 15. They can be derived analytically because the integration on the volume of the element is trivial.

$$\mathbf{K}_u = E_t\, A\, \frac{L^2}{L_0^3} \begin{bmatrix} 1 & 0 & 0 & -1 & 0 & 0 \\ & 0 & 0 & 0 & 0 & 0 \\ & & 0 & 0 & 0 & 0 \\ & & & 1 & 0 & 0 \\ & \text{SYM} & & & 0 & 0 \\ & & & & & 0 \end{bmatrix} \qquad (14)$$

$$\mathbf{K}_S = S_{xx}\frac{A}{L_0}\begin{bmatrix} 1 & 0 & 0 & -1 & 0 & 0 \\ & 1 & 0 & 0 & -1 & 0 \\ & & 1 & 0 & 0 & -1 \\ & & & 1 & 0 & 0 \\ & \text{SYM} & & & 1 & 0 \\ & & & & & 1 \end{bmatrix} \quad (15)$$

The Beam Finite Element

The element has a constant section along the longitudinal axis that is a straight line extending between the two end nodes; this line joining the two end nodes is called the "node line" in this paper. Each of these two end nodes has seven degrees of freedom: three translations, three rotations, and warping. A central node has been added bearing the nonlinear component of the longitudinal displacement. This has been done in order to avoid the excessive stiffness that can develop in the element when the zones with nonlinear material behavior are not symmetrically distributed on the depth of the section. Practically speaking, if this additional degree of freedom is not present, the location of the points that have a zero strain is, in a 2D case, systematically a line that is parallel to the node line. This additional degree of freedom allows a solution in which this line of zero strain is not parallel to the longitudinal axis which means that, for example, the extension of plasticity on the depth of the section is changing along the axis of the element.

The position in the section of the node line that connects the elements is arbitrarily chosen by the user. The software does not include the notion of center of gravity (this position is changing continuously during the fire). This means that the beam element is of the "stiffener" type.

The Bernoulli hypothesis is used in the derivation of the strains; plane sections remain plane in bending. As a consequence, this element will not be able to track shear failure modes.

The hypothesis of Von Karman is used: the strains are small. See Equation 16.

$$\frac{\partial u}{\partial x} \ll 1 \quad (16)$$

The rotations are assumed to be small (note that they are evaluated in the co-rotated configuration). See Equation 17.

$$\sin\alpha \cong \alpha; \quad \cos\alpha \cong 1 \quad (17)$$

The hypothesis of Vlassov is used; in pure torsion, the section undergoes warping, the amplitude of which is proportional to the increase of the angle of torsion.

The strains are normally defined by Equations 18.

$$\begin{aligned} E_{xx} &= u' - y\left(v'' - z_c\psi''\right) - z\left(w'' + y_c\psi''\right) \\ &\quad - yw''\psi + zv''\psi - \omega\psi'' \\ &\quad + \frac{1}{2}\left(v'^2 + w'^2 + \left[y^2 + z^2\right]\psi'^2\right) \\ E_{xy} &= -\frac{1}{2}\psi'\left(z - z_c + \frac{\partial\omega}{\partial y}\right); \\ E_{xz} &= \frac{1}{2}\psi'\left(y - y_c + \frac{\partial\omega}{\partial z}\right) \end{aligned} \quad (18)$$

where

u, v, w	=	displacements of the node line, expressed as functions of the nodal displacements via polynomial shape functions (third order for the v and w, second order for u)
ψ	=	rotation along the longitudinal axis, expressed as a function of the nodal displacements via third order polynomial shape functions
ω	=	warping function
y, z	=	coordinates in the section
y_c, z_c	=	coordinates of the center of torsion in the section, introduced by the user

As such, Equations 18 in fact introduce some locking, or excessive stiffness, in the element because the terms of the axial strain that have the same order in y or z have not the same order in x and it is thus not possible to have a correct representation of the pure bending mode. In order to avoid this locking, it has been proposed by de Ville (1988) to replace the terms in v'^2 and w'^2 by their average value on the length of the element in order to give them the same order in x as the term u'. Similarly, the coupling terms in $w''\psi$ and $v''\psi$ are replaced by a linear function in x, which gives them the same degree as the terms in v'', w'' and ψ''. This linear function is the one that minimizes the difference with the exact function and it is obtained by the least square method. When calculating the variation of the strain, some additional terms have to be added in order to ensure that the six rigid body modes do not produce any strain.

These modifications to the strain yield an element that is free of locking, and in which the nodal forces that result from the integration of the internal stresses are in equilibrium, which ensures convergence. More information is given by Franssen (1997).

The integration of the longitudinal stresses and stiffness on the section is based on the fiber model; the section is supposed to be made of a certain number of parallel fibers. In fact, the same discretization as the one used for the thermal analysis is used. Each finite element of the thermal analysis, with its known material type and temperature, is considered as a fiber. The integration is then done very easily according

to Equations 19, for example, for a 2D element.

$$N = \sum_i \sigma_i A_i; \quad M_y = \sum_i \sigma_i y_i A_i$$
$$EA = \sum_i E_i A_i; \quad ES_y = \sum_i E_i y_i A_i; \quad EI_y = \sum_i E_i y_i^2 A_i \tag{19}$$

The integrations along the longitudinal axis are performed by a numerical integration of Gauss, with the user choosing the number of points to be used. Integration between two points has proved to be a good choice, but more can be adopted.

The integration of the term accounting for torsion yields the following quantity that is the stiffness in torsion.

$$GC_t = \int_\Omega G\left[\left(y - y_c + \frac{\partial \omega}{\partial z}\right)^2 + \left(z - z_c + \frac{\partial \omega}{\partial y}\right)^2\right] d\Omega \tag{20}$$

This quantity is in fact evaluated once in a preliminary calculation by SAFIR and then it is supposed to not vary during the mechanical analysis (the user can arbitrarily reduce the calculated value in order to take into account, for example, the effects of cracking in a concrete section or the effects of high temperatures in a steel section). To rely on the notion of torsional stiffness allows the use of uniaxial stress-strain relationships in the beam element, but the element will not be appropriate for the modeling of structures in which torsion is the dominant load path, which is not very often the case in building structures.

A validation of the beam finite element, at least in 2D situations, was performed by Franssen (1994).

The Shell Finite Element

The element is a quadrangle based on four nodes, each bearing three translations and three rotations. Figure 4 shows the local axes x and y. The axis z is perpendicular to the medians ac and bd.

For the membrane behavior, the classical quadratic membrane displacement field is enlarged to cubic degree by means of cubic (along ξ and η) functions and constants A_{ij}. The development is similar to the one found by Allman (1984) for a triangular element.

$$u = \frac{1}{4}\left[\sum_{k=1}^{4}(1+\xi\xi_k)(1+\eta\eta_k)u_k + \sum_{sides}\phi_{ij}l_{ij}\cos\gamma_{ij}\left(\omega_j - \omega_i\right) + \sum_{sides}\psi_{ij}l_{ij}\cos\gamma_{ij}\,A_{ij}\right]$$
$$v = \frac{1}{4}\left[\sum_{k=1}^{4}(1+\xi\xi_k)(1+\eta\eta_k)v_k + \sum_{sides}\phi_{ij}l_{ij}\sin\gamma_{ij}\left(\omega_j - \omega_i\right) + \sum_{sides}\psi_{ij}l_{ij}\sin\gamma_{ij}\,A_{ij}\right] \tag{21}$$

with

$$\phi_{12} = \frac{1}{16}(1-\xi^2)(1-\eta)$$
$$\phi_{23} = \frac{1}{16}(1+\xi)(1-\eta^2)$$
$$\phi_{34} = \frac{1}{16}(1-\xi^2)(1+\eta)$$
$$\phi_{41} = \frac{1}{16}(1-\xi)(1-\eta^2)$$
$$\psi_{12} = \frac{1}{8}(1-\xi^2)(1-\eta)\xi\eta^2 \tag{22}$$
$$\psi_{23} = \frac{1}{8}(1+\xi)(1-\eta^2)\xi^2\eta$$
$$\psi_{34} = -\frac{1}{8}(1-\xi^2)(1+\eta)\xi\eta^2$$
$$\psi_{41} = -\frac{1}{8}(1-\xi)(1-\eta^2)\xi^2\eta$$

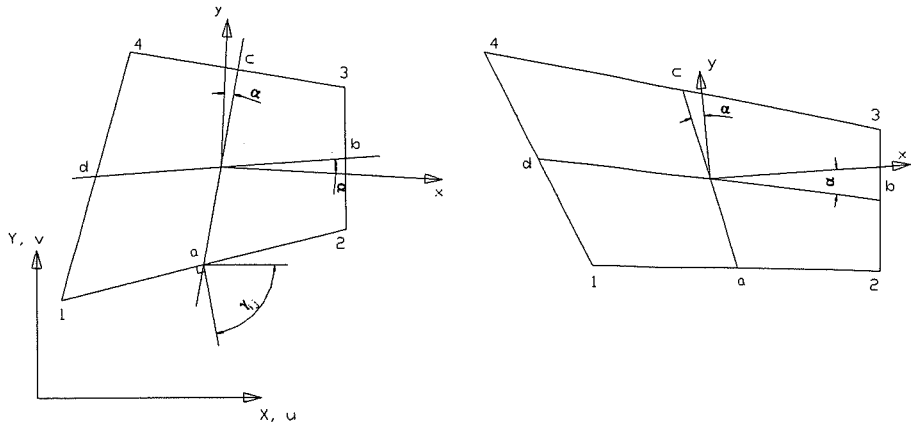

Fig. 4. Local system of coordinates in the shell element.

$$l_{ij} = \sqrt{\left(x_j - x_i\right)^2 + \left(y_j - y_i\right)^2} \tag{23}$$

$$A_{ij} = \frac{\omega_i + \omega_j}{2} + \frac{B_{ij} + B_{ji}}{2} \tag{24}$$

ω_i is the rotation at node i and γ_{ij} is the direction of the outward normal along the edge ij. The coefficients B_{ij} are defined by Jaamei (1988) and the functions ψ_{ij} are chosen so as to be orthogonal to ϕ_{ij} with respect to integration over the quadrangle and, finally, the shear strains are assumed to be constant over the element in order to improve the convergence.

The behavior in bending is according to the classical formulation of the Discrete Kirchoff Quadrangle (DKQ). See, for example, Batoz and Ben Tahar (1982).

Integration on the section is numerically done by four points of Gauss whereas the user can choose the number of Gauss points that are used for the numerical integration on the thickness, from two if the membrane behavior is dominant to ten if bending is dominant.

For steel plates, a plane stress Von Mises plasticity model has been implemented with the variation of the Young's modulus as a function of temperature following the recommendations of Eurocode 3 (Eurocode, 1995c), the Poisson ratio being constant, and an elliptical curve for the isotropic hardening that matches as closely as possible the Eurocode 3 uniaxial stress-strain relationship. See Figure 5.

For reinforced concrete plates, the contribution of the plain concrete is taken into account also by a Von Mises plane stress plasticity model on which a Rankine tension cut off has been added in tension. The evolution of the Young's modulus and the curve for the isotropic hardening are also chosen in order to match as closely as possible the recommendations of Eurocode 2 (1995b) for the uniaxial stress-strain relationship of concrete.

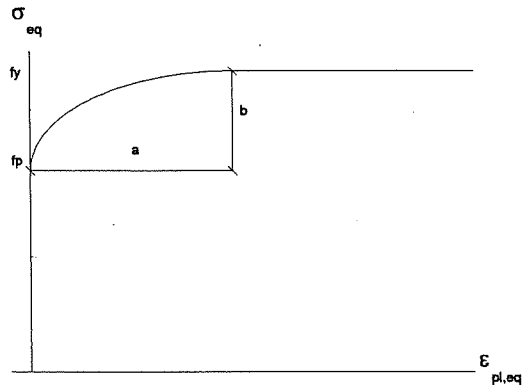

Fig. 5. Hardening curve for the steel plane stress model.

The steel reinforcements are smeared laterally and their contribution is taken into account by a uniaxial model; only an elongation in the direction of their axis will produce a stress while an elongation perpendicular to the axis or a shear strain in the element do not produce any stress in the bars.

More information as well as validation examples on the shell element are given by Talamona and Franssen (2000).

Capabilities and Limitations of the Software

Different element types can be mixed in a single mechanical analysis. Master-slave relationships can be introduced between selected degrees of freedom of defined nodes. Applied forces as well as displacements at selected degrees of freedom can be forced to follow any function of time defined by the user. Different strategies are available to rearrange the order of the equations in order to reduce memory requirements as well as CPU time; this rearrangement is transparent to the user. When convergence is not obtained at a given time, it is possible for the software to come back automatically to the last converged time and make a new attempt with a reduced time step. The software is written in FORTRAN language making use of dynamic memory allocation so that there is no restriction embedded in the code on the number of nodes, elements, or materials. All variables are stored in the central memory, unless the operating system of the computer detects the need to swap to the disk.

A preprocessor with a graphic interface has been written in VisualBasic but its capabilities are limited to the preparation of input files for 2D thermal analyses in sections based on H steel sections. The data for other structures have to be prepared with a text editor or with one of the meshing software programs available on the web. A graphic postprocessor is also available that allows viewing, saving and printing the initial or deformed shape of the structure, various diagrams of effects of actions, isotherms in the structure, or the evolution of various results as a function of time.

The main limitations of the software and of this type of SiF modeling are listed hereafter:

- Spalling in concrete cannot be predicted by this type of software.
- Because it is based on the Bernoulli hypothesis, the beam finite element cannot detect failure by local buckling, by slip between concrete and the re-bars or shear failure.
- The strategy of successive static analyses can in some cases prevent the simulation from running further than a certain moment in the fire because a negative stiffness appears locally in one part of the structure whereas the overall stability of the total structure is not yet endangered. This is the case, for example, when a restrained column exhibits buckling in a moment resisting frame. Recent work performed in Liege now allows the simulations to

run beyond these moments of local failure provided that the user has chosen to make a dynamic mechanical analysis. See Franssen (2004).

- Structures that are very large numerically cannot yet be analyzed as a whole by this type of non-linear model because, although they increase continuously, the capabilities of the computers are still limited (as well as the time allocated to the user to create his model).

- Because of that, sub structures are very often considered, but the sensitivity of the result to the choice made for the boundary conditions should normally be checked in every case.

- This type of software tends to be very ductile in some cases and it is then the responsibility of the user to define the ultimate limit state; what is acceptable in terms of deformation and what is not?

Examples

Figure 6 shows the deflected shape just before failure of a steel frame in an industrial building modeled with beam and truss finite elements. It has been assumed in this analysis that only this frame was subjected to the fire. The result may, of course, be significantly influenced by the assumptions made for the boundary conditions, especially for the elongation of the purlins.

Figure 7 shows the deformed shape of a steel section that is subjected to a temperature increase and to an imposed shortening. The deformation has not been amplified in the drawing and, although it is not yet as large as the one that can be observed in certain tests (see Figure 8), or in real fires, it shows that the element has good capabilities in terms of numerical ductility.

The next example is a reinforced concrete slab tested in New Zealand (Lim, 2003). This is a 4 by 3 m² slab. One quarter of the slab has been analyzed for symmetry reasons. The slab is supported on four perimeter steel beams, themselves supported at the corners of the assembly. Figure 9 shows the deformed shape after more than three hours in the fire test. The deflection is close to 300 mm, in other words, $L/10$.

It is possible to explain such a long fire resistance in this unrestrained slab, in fact far beyond the fire resistance time predicted by the theory of ultimate bending moment failure lines, only if the effect of membrane forces is taken into account. These forces as computed by SAFIR can be seen in Figure 10.

THE TORSION ANALYSIS

As mentioned previously, it is necessary to introduce a value of the torsional stiffness as one of the properties of the section when using a 3D beam finite element. Except for simple cases, this value is not known to the user. SAFIR allows the user to compute the value of the elastic torsional stiffness of any composite section by solving Equation 25 written in a displacement formulation on the section.

$$W = \bar{\theta}^2 \int_{\Omega} G\left(\delta\omega_{,z}\,\omega_{,z} + \delta\omega_{,y}\,\omega_{,z} + \delta\omega_{,y}\,z - \delta\omega_{,z}\,y\right) d\Omega = 0 \quad (25)$$

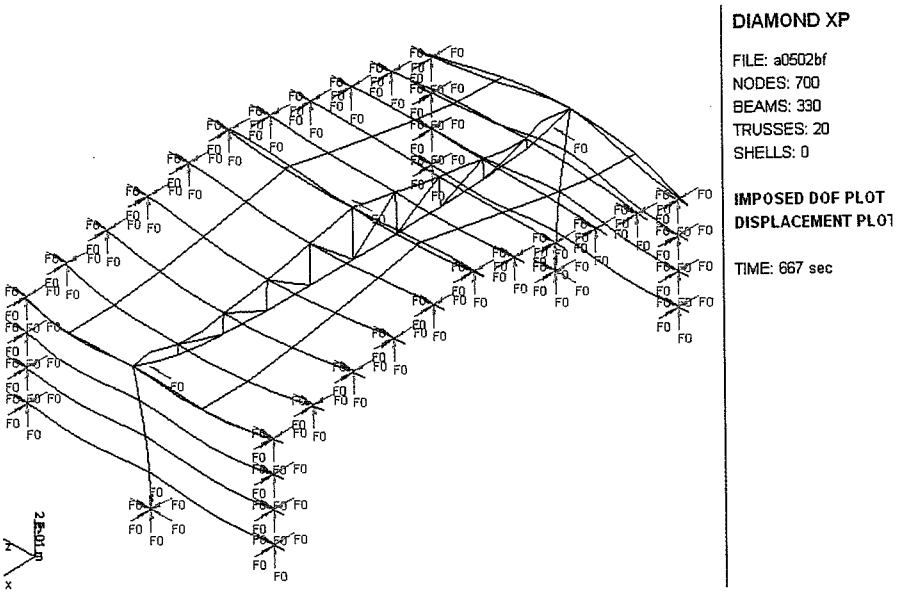

Fig. 6. Failure in an industrial steel building.

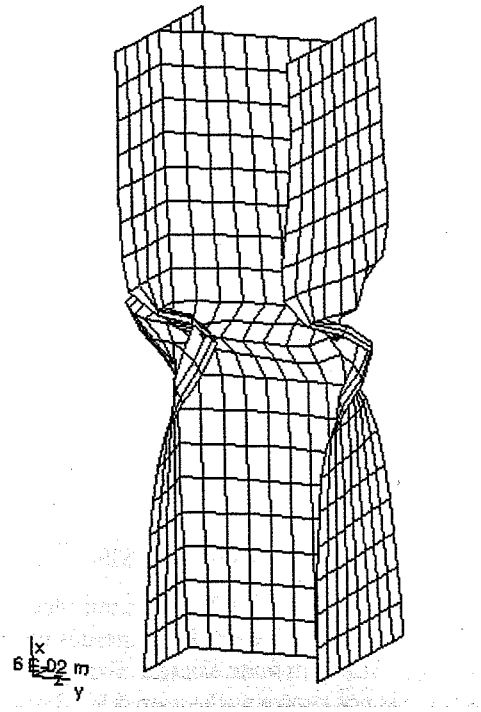

Fig. 7. Local buckling in a steel section.

Fig. 8. Local buckling observed at Cardington (test by BRE).

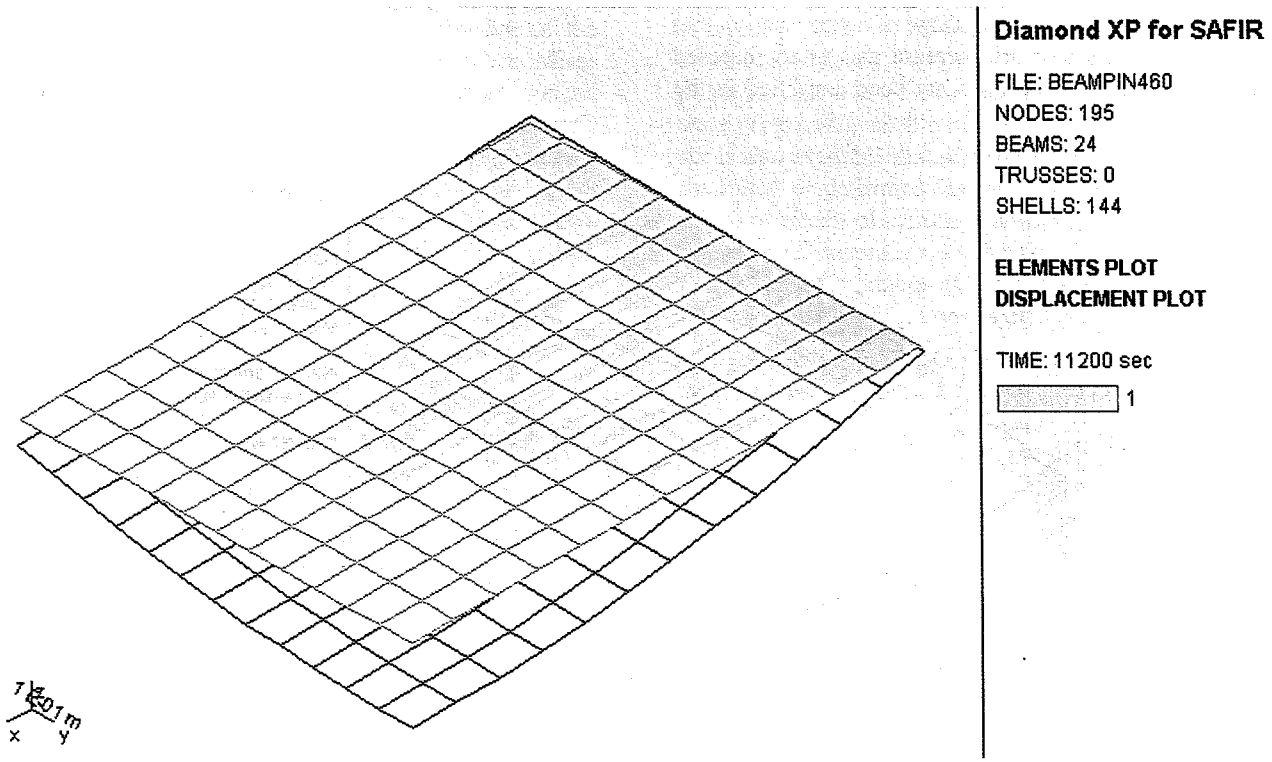

Fig. 9. Displacements in the slab.

where

$\bar{\theta}$ = variation of rotation along the longitudinal axis
G = shear modulus of the material
ω = warping function

The same discretization as the one used for the thermal analysis can be used for representing the section as well as the solution ω in the finite element analysis. The matrix system of equations that is derived from Equation 25 has to be solved only once.

Once the warping function has been computed, the torsional stiffness is evaluated from Equation 26.

$$GC_t = \int_{\Omega} G\left(\omega_{,y}\, z - \omega_{,z}\, y + y^2 + z^2\right) d\Omega \qquad (26)$$

As mentioned in a previous section, the user has the opportunity to reduce the computed value in order to take into account either the effect of elevated temperatures (de Souza Junior, 2002) or the effect of cracking in concrete. Some engineering judgment is required here.

COLLABORATION AND POLICY OF DEVELOPMENT

The desire of the author is that the utilization of this computer code does not remain confined to the department where it has been developed. This is why a limited version is freely available for education or demonstration purposes.

University departments or research centers willing to use it for research purposes can receive a copy of the full version on the condition that whatever new feature is developed is transmitted to the University of Liege for introduction in the next version for the benefit of the whole community.

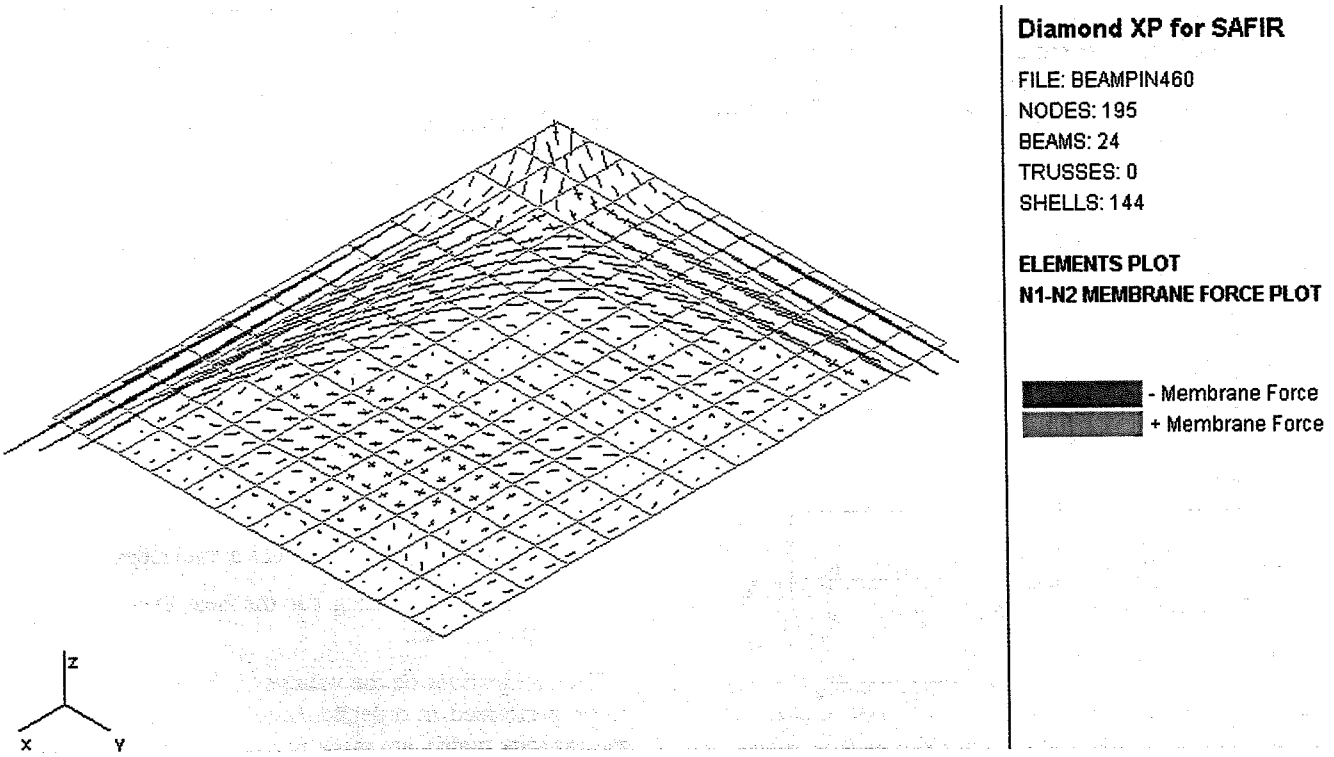

Fig. 10. Membrane forces in the slab.

APPENDIX

The local equation describing conduction in solid materials has the form of Equation 1 in a Cartesian system of coordinates.

$$k\left(\frac{\partial^2 T}{\partial x^2}+\frac{\partial^2 T}{\partial y^2}+\frac{\partial^2 T}{\partial z^2}\right)+Q-C\rho\frac{\partial T}{\partial t} = 0 \qquad (1)$$

where

k	=	thermal conductivity, W/mK
T	=	temperature, K
x, y, z	=	coordinates, m
Q	=	internally generated heat, W/m³
C	=	specific heat, J/kgK
ρ	=	specific mass density, kg/m³
t	=	time, s

The classical shape functions are used. See for example Equation 2 for a triangular element or Equation 3 for a rectangular element, in which ξ and η are the parametric coordinates of the reference elements as defined in Figure 11.

$$\mathbf{N} = \langle 1-\xi-\eta\,;\,\xi\,;\,\eta\rangle \qquad (2)$$

$$\mathbf{N} = \frac{1}{4}\left\langle \begin{matrix}(1-\xi)(1-\eta)\,;\,(1+\xi)(1-\eta)\,;\\ (1+\xi)(1+\eta)\,;\,(1-\xi)(1+\eta)\end{matrix}\right\rangle \qquad (3)$$

The shape functions allow the geometry to be represented as a function of the coordinates of the nodes according to Equations 4 and the temperature at any point as a function of the temperature of the nodes according to Equation 5. These functions ensure temperature continuity at the boundaries between adjacent elements; there is no gap or overlap in the material between adjacent elements and the temperature at a common border is the same in both elements. The temperature in fact varies linearly on all the borders of the elements. The first derivative of the temperature perpendicular to the border is not continuous which means that the heat flux is not continuous from one element to the other.

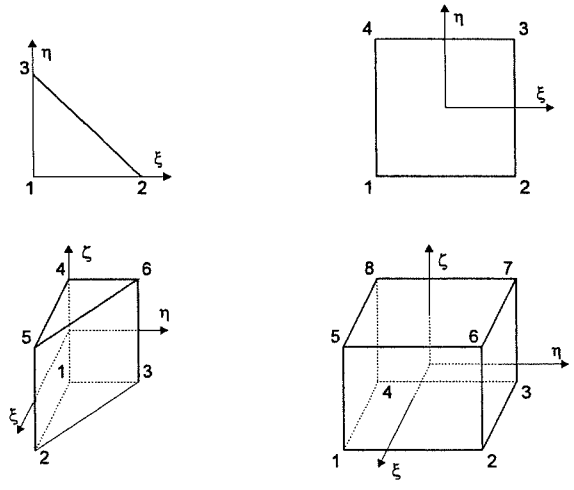

Fig. 11. Reference elements and parametric coordinates.

$$x = N_i\,x_i;\; y = N_i\,y_i;\; z = N_i\,z_i \qquad (4)$$

$$T = N_i T_i \qquad (5)$$

The local form of Equation 1 is transformed into a form that is suitable for the finite element method by first replacing the temperature by the approximation of Equation 5 in Equation 1. The equation is then multiplied by a weighting function and integrated on the volume of the element; this is the weighted residual method which is called the Galerkin method in the particular case where the shape functions used for describing the geometry are also used as the weighting functions. If the first term is transformed by the Green equation and if the boundary condition described by Equation 6 is used, Equation 1 is transformed into Equation 7.

$$q_n = -k\nabla T_j\,N_j \qquad (6)$$

$$\int_{element} k\{\nabla N_i\}\langle\nabla N_j\rangle dV\,T_i + \int_{element} C\rho N_i N_j\,dV\,\dot{T}_i + \int_{element} Q N_j\,dV = -\int_{boundary} N_j\,q_n\,dS \qquad (7)$$

where ∇ means $\langle\partial/\partial x;\ \partial/\partial y;\ \partial/\partial z\rangle$ and q_n is the heat flux at the boundary of the element.

Finally, when the contributions from all the elements are summed, the matrix Equation 8 is obtained, describing the equilibrium of heat fluxes in the structure at any given instant in time.

$$[K]\{T\}+[C]\{\dot{T}\}=\{g\} \qquad (8)$$

where

[K]	matrix of conductivity,
[C]	matrix of capacity,
$\{\dot{T}\}$	vector of the temperatures at the nodes,
{g}	vector accounting for the heat exchanges at the boundaries.

The integrations on the volume of the elements that have to be performed in order to evaluate the conductivity and the capacity matrix are made numerically by the method of Gauss and the user can choose the number of points of integration, typically 2 × 2 points for a 4 noded 2D element. The fact that the thermal properties are temperature dependent

is taken into account, including the fact that these thermal properties vary in the element, in other words, from one point of integration to another.

Equation 8 expresses the thermal equilibrium at a given time; it has to be integrated in time in order to yield the evolution of the temperatures during the course of the fire. This is done in SAFIR by the implicit single step scheme of the generalized central point briefly described hereafter.

It is assumed that the nodal temperatures vary linearly with time from one time step to the next one. If $\mathbf{T}_n$ is the known solution at time t_n, and $\mathbf{T}_{n+1}$ is the solution aimed for at the next time t_n, this hypothesis is expressed by Equation 9.

$$\mathbf{T}_\theta = \mathbf{T}_n + \theta\,(\mathbf{T}_{n+1} - \mathbf{T}_n) \tag{9}$$

with $\theta \in [0,1]$ to be chosen by the user.

The first derivative of the temperature is then a constant, given by Equation 10.

$$\dot{\mathbf{T}}_\theta = \frac{\mathbf{T}_\theta - \mathbf{T}_n}{\theta\,\Delta t} \tag{10}$$

with $\Delta t = t_{n+1} - t_n$ also chosen by the user.

A first approximation of the solution at time $t_\theta = t_n + \theta\Delta t$ can easily be obtained by linear extrapolation of the results obtained at the two previous time steps as can be seen on Figure 12 drawn for a system with one single temperature. If this first solution, noted $\mathbf{T}_\theta^1$ were the exact solution, it would satisfy Equation 8.

As this is not the exact solution, there is a residue, an out of balance thermal force, given by Equation 11 if Equation 10 is introduced in Equation 8.

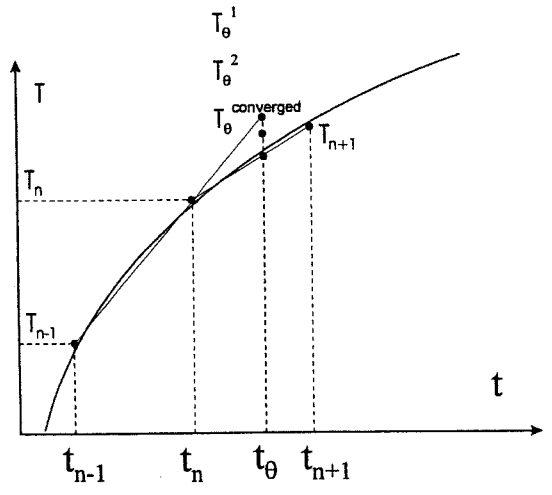

Fig. 12. Iteration process in the thermal analysis.

$$\mathbf{r}\left(\mathbf{T}_\theta^1\right) = \mathbf{K}\,\mathbf{T}_\theta^1 + \mathbf{C}\frac{\mathbf{T}_\theta^1 - \mathbf{T}_n}{\theta\,\Delta t} - \mathbf{g} \neq \mathbf{0} \tag{11}$$

The correction $\Delta\mathbf{T}_\theta^1$ that has to be applied in order to improve this first approximation of the solution $\mathbf{T}_\theta^1$ is obtained by expressing the new residue by a linearization of Newton and expressing that it should be equal to zero (see Equation 12):

$$\mathbf{r}\left(\mathbf{T}_\theta^2\right) = \mathbf{r}\left(\mathbf{T}_\theta^1 + \Delta\mathbf{T}_\theta^1\right) = \mathbf{r}\left(\mathbf{T}_\theta^1\right) + \frac{\partial \mathbf{r}}{\partial \mathbf{T}}\Delta\mathbf{T}_\theta^1 = \mathbf{0} \tag{12}$$

hence

$$\Delta\mathbf{T}_\theta^1 = -\frac{\partial \mathbf{r}}{\partial \mathbf{T}}^{-1}\,\mathbf{r}\left(\mathbf{T}_\theta^1\right) \tag{13}$$

The first derivative of the residue is obtained from Equation 11.

$$\frac{\partial \mathbf{r}}{\partial \mathbf{T}} \cong \mathbf{K} + \frac{\mathbf{C}}{\theta\,\Delta t} - \frac{\partial \mathbf{g}}{\partial \mathbf{T}} \tag{14}$$

Some approximations have been made in order to obtain a symmetric matrix when establishing Equation 14; the terms in $\partial\mathbf{K}/\partial\mathbf{T}$ and $\partial\mathbf{C}/\partial\mathbf{T}$ have been neglected and the term $\partial\mathbf{g}/\partial\mathbf{T}$ has been rendered symmetric. The convergence toward the solution may thus require a few more iterations than would be the case if the exact iteration matrix would be used, but the advantages of using a symmetric matrix, in term of required storage capacity and in terms of CPU time, by far outweigh the time spent by possible additional iterations. What is very important is that the convergence is toward the true solution. This is because convergence is evaluated via the residue and the approximations do not influence this residue (see Equation 11).

The iteration process is repeated until the residue and/or the corrections made on the temperatures reach an acceptable low level. The temperatures at the end of the time step are directly obtained by linear extrapolation from the solutions at t_n and t_θ.

REFERENCES

Allman, D.J. (1984), "A Compatible Triangular Element Including Vertex Rotations For Plane Elastic Analysis," *Computers & Structures*, Vol. 19, pp 1-8.

Batoz, J.L., and Ben Tahar, M. (1982), "Evaluation of a New Quadrangular Thin Plate Bending Element," *International Journal of Numerical Methods in Engineering*, Vol. 18, pp. 1655-1677.

Becker, J., Bizri, H., and Bresler, B. (1974a), *Fires-R.C. A Computer Program for the Fire Response of Structures—Thermal*, Report No. UCB FRG 74-1, University of California, Berkeley.

Becker, J., Bizri, H., and Bresler, B. (1974b), *Fires-T. A Computer Program for the Fire Response of Structures—Reinforced Concrete*, Report No. UCB FRG 74-3, University of California, Berkeley.

Coin, A. (1976), *Températures dans un solide hétérogène au cours d'un incendie*, Annales de l'Inst. Techn. Du Bâtiment et des Travaux Publics, Série Informatique Appliquée, No. 28.

De Ville de Goyet, V. (1988), *L'analyse Statique Non Linéaire par la Méthode des éléments Finis des Structures Formées de Poutres à Section Non Symétriques*, Ph.D. thesis, University of Liege, F.S.A.

De Souza Junior, V., and Franssen, J.-M. (2002), "Lateral Buckling of Steel I-Beams at Elevated Temperature—Comparison between the Modelling with Beam and Shell Elements," *Proceedings Third European Conference on Steel Structures*, ISBN: 972-98376-3-5, Coïmbra, University de Coïmbra, A. Lamas & L. Simoes da Silva ed., pp. 1479-1488.

Dotreppe, J.-C. (1972), *Etude par éléments Finis des Dalles en Béton Armé Jusqu'à la Ruine*, Ph.D. thesis, F.S.A., University of Liege.

Dotreppe, J.-C. (1980), *Méthodes Numériques pour la Simulation du Comportement au Feu des Structures en Acier et en Béton Armé*, Thèse d'agr. Ens. Sup., F.S.A., University of Liege.

Eurocode (1995a), *Eurocode 1: Basis of design and actions on structures—Part 2-2: Actions on Structures—Actions on Structures Exposed to Fire*, ENV 1991-2-2, CEN, Brussels, February.

Eurocode (1995b), *Eurocode 2: Design of Concrete Structures, Part 1.2: General Rules, Structural Fire Design*, ENV 1992-1-2, CEN, Brussels, Novembre.

Eurocode (1995c), *Eurocode 3: Design of Steel Structures, Part 1.2: General Rules, Structural Fire Design*, ENV 1993-1-2, CEN, Brussels, May.

Eurocode (1998), *Eurocode 9: Design of Aluminium Alloy Structures, Part 1-2: Structural Fire Design*, ENV 1999-1-2, CEN, Brussels, May.

Franssen, J.-M. (1987), *Etude du Comportement au Feu des Structures Mixtes Acier-Béton*, Collection des Publications de la F.S.A. de l'Univ. de Liège, No. 111.

Franssen, J.-M., Schleich, J.-B., Cajot, L.-G., Talamona, D., Zhao, B., Twilt, L., and Both, K. (1994), "A Comparison Between Five Structural Fire Codes Applied to Steel Elements," *Proceedings of Fourth International Symposium on Fire Safety Science*, Ottawa, Kashiwagi, T., ed., Gaithersburg, pp. 1125-1136.

Franssen, J.-M. (1997), *Contributions à la Modélisation des Incendies Dans les Bâtiments et de Leurs Effets sur les Structures*, Thèse d'agrégation, University of Liege, F.S.A.

Franssen, J.-M. (2003), *Heat Transfer by Radiation in Internal Cavities With a Complex Shape*, ASCE/SFPE Specialty Conference on Designing Structures for Fire, Baltimore, MD, October.

Franssen, J.-M. (2004), "Dynamic Analysis Used to Cope With Partial and Temporary Failures," *Proceedings of Third International SiF Workshop*, Franssen, Benichou, Kodur & Sultan Ed., NRC-CNRC, Ottawa.

Hottel, H.C. (1954), "Radiant Heat Transmission," in William H. McAdams (ed.), *Heat Transmission*, 3rd ed., pp. 55-125, McGraw-Hill Book Co., New York.

Iding, R., Bresler, B., and Nizamuddin, Z. (1977a), "FIRES-T3, A Computer Program for the Fire Response of Structures—Thermal," *Report UCB FRG 77-15*, University of California, Berkeley.

Iding, R., Bresler, B., and Nizamuddin, Z. (1977b), "FIRES-RCII, A Computer Program for the Fire Response of Structures—Reinforced Concrete Frames," *Report UCB FRG 77-8*, University of California, Berkeley.

Iding, R., and Bresler, B. (1980), *Analysis of Fire Response of Steel Floor Systems*, Wiss, Janney, Elstner & Associates, Inc.

ISO (1999), *Fire-resistance tests—Elements of Building Construction—Part 1: General Requirements*, ISO 834-1:1999, Geneva.

Jaamei, S. (1988), "JET Thin Shell Finite Element with Drilling Rotations," *IREM Internal Report 88/7*, Swiss Federal Institute of Technology, Lausanne, Switerland, July.

Lim, L. (2003), *Membrane Action in Fire Exposed Concrete Floor Systems*, Ph.D. thesis (in preparation), Department of Civil Engineering, University of Canterbury.

Pintea, D., and Franssen, J.-M. (1997), "Evaluation of the Thermal Part of the Code SAFIR by Comparison With the Code TASEF," *Proceedings of the Eighth International Conference on Steel Structures*, Volume 2, M. Ivan ed., MIRTON, Timisoara, pp. 636-643.

Schleich, J.-B., Dotreppe J.-C., and Franssen J.-M. (1986), "Numerical Simulations of Fire Resistance tests on steel and composite structural elements or frames," *Proceedings of the First International Symposium on Fire Safety Science*, Hemisphere Publishing Corporation, pp. 311-323.

Talamona, D., and Franssen, J.-M. (2000), "New quadrangular shell element in SAFIR," *Proceedings First International "Structures in Fire" Workshop*, Copenhagen, J.M. Franssen ed., Liège, pp. 195-210.

Tien, C.L., Lee, K.Y., and Stretton, A.J. (1995), "Radiation Heat Transfer," *The SFPE Handbook of Fire Protection Engineering*, SFPE, Boston, pp. 1,65-1,79.

Wickström, U. (1979), "A Numerical Procedure for Calculating Temperature in Hollow Structures Exposed to Fire," *Report No. 79-2*, Department of Structural Mechanics, Lund, Sweden.